

Intracranial EEG Structure-Function Coupling and Seizure Outcomes After Epilepsy Surgery

Nishant Sinha, PhD, John S. Duncan, FRCP, FMedSci, Beate Diehl, PhD, Fahmida A. Chowdhury, PhD, Jane de Tisi, BA, Anna Miserocchi, FRCS (SN), Andrew William McEvoy, FRCS (SN), Kathryn A. Davis, MD, MSCE, Sjoerd B. Vos, PhD, Gavin P. Winston, BM BCh, PhD, FRCP, Yujiang Wang, PhD, and Peter Neal Taylor, PhD

Neurology® 2023;101:e1293-e1306. doi:10.1212/WNL.0000000000207661

Correspondence

Dr. Sinha
nishant.sinha@pennmedicine.upenn.edu
or Dr. Taylor
peter.taylor@newcastle.ac.uk

Abstract

Background and Objectives

Surgery is an effective treatment for drug-resistant epilepsy, which modifies the brain's structure and networks to regulate seizure activity. Our objective was to examine the relationship between brain structure and function to determine the extent to which this relationship affects the success of the surgery in controlling seizures. We hypothesized that a stronger association between brain structure and function would lead to improved seizure control after surgery.

Methods

We constructed functional and structural brain networks in patients with drug-resistant focal epilepsy by using presurgery functional data from intracranial EEG (iEEG) recordings, presurgery and postsurgery structural data from T1-weighted MRI, and presurgery diffusion-weighted MRI. We quantified the relationship (coupling) between structural and functional connectivity by using the Spearman rank correlation and analyzed this structure-function coupling at 2 spatial scales: (1) global iEEG network level and (2) individual iEEG electrode contacts using virtual surgeries. We retrospectively predicted postoperative seizure freedom by incorporating the structure-function connectivity coupling metrics and routine clinical variables into a cross-validated predictive model.


Results

We conducted a retrospective analysis on data from 39 patients who met our inclusion criteria. Brain areas implanted with iEEG electrodes had stronger structure-function coupling in seizure-free patients compared with those with seizure recurrence ($p = 0.002$, $d = 0.76$, area under the receiver operating characteristic curve [AUC] = 0.78 [95% CI 0.62–0.93]). Virtual surgeries on brain areas that resulted in stronger structure-function coupling of the remaining network were associated with seizure-free outcomes ($p = 0.007$, $d = 0.96$, AUC = 0.73 [95% CI 0.58–0.89]). The combination of global and local structure-function coupling measures accurately predicted seizure outcomes with a cross-validated AUC of 0.81 (95% CI 0.67–0.94). These measures were complementary to other clinical variables and, when included for prediction, resulted in a cross-validated AUC of 0.91 (95% CI 0.82–1.0), accuracy of 92%, sensitivity of 93%, and specificity of 91%.

Discussion

Our study showed that the strength of structure-function connectivity coupling may play a crucial role in determining the success of epilepsy surgery. By quantitatively incorporating

MORE ONLINE

 **Class of Evidence**
Criteria for rating therapeutic and diagnostic studies
[NPub.org/coe](https://www.ncbi.nlm.nih.gov/pmc/articles/PMC10488888/)

From the Department of Neurology (N.S., K.A.D.), Penn Epilepsy Center, Perelman School of Medicine, and Center for Neuroengineering and Therapeutics (N.S., K.A.D.), University of Pennsylvania, Philadelphia; Translational and Clinical Research Institute (Y.W., P.N.T.), Faculty of Medical Sciences, and Computational Neuroscience, Neurology, and Psychiatry Lab (Y.W., P.N.T.), ICOS Group, School of Computing, Newcastle University; Department of Epilepsy (J.S.D., B.D., F.A.C., J.d.T., A.M., A.W.M., G.P.W., Y.W., P.N.T.), UCL Queen Square Institute of Neurology; UCL Centre for Medical Image Computing (S.B.V.); Neuroradiological Academic Unit (S.B.V.), UCL Queen Square Institute of Neurology, London; MRI Unit (J.S.D., G.P.W.), Chalfont Centre for Epilepsy, Bucks, United Kingdom; Centre for Microscopy, Characterisation, and Analysis (S.B.V.), The University of Western Australia, Nedlands; and Division of Neurology (G.P.W.), Department of Medicine, Queen's University, Kingston, Canada.

Go to [Neurology.org/N](https://www.neurology.org/N) for full disclosures. Funding information and disclosures deemed relevant by the authors, if any, are provided at the end of the article.

Glossary

AUC = area under the receiver operating characteristic curve; ECOG = electrocorticography; FC = functional connectivity; iEEG = intracranial EEG; ILAE = International League Against Epilepsy; NHNN = National Hospital for Neurology and Neurosurgery; SC = structural connectivity; SEEG = stereotactic EEG; SVM = support vector machine.

structure-function coupling measures and standard-of-care clinical variables into presurgical evaluations, we may be able to better localize epileptogenic tissue and select patients for epilepsy surgery.

Classification of Evidence

This is a Class IV retrospective case series showing that structure-function mapping may help determine the outcome from surgical resection for treatment-resistant focal epilepsy.

Introduction

Surgery is an effective therapy for treating focal drug-resistant epilepsy. Accurate localization and complete removal of the epileptogenic tissues are essential for achieving seizure freedom.¹ However, localizing these tissues can sometimes be challenging using noninvasive methods. To aid in localization, intracranial EEG (iEEG) electrodes are implanted directly in contact with the cortex.² Unfortunately, even after iEEG implantation and surgery, 30%–40% of patients continue to experience seizures.³ This is often due to remaining epileptogenic tissues, which cause seizure recurrence.⁴ Reasons for incomplete resection include (1) incomplete or missed localization, (2) proximity to the eloquent cortex precluding complete resection, or (3) a combination of both factors.⁴ Growing evidence suggests that epileptogenic tissue may constitute a distributed network^{5–7} rather than a well-circumscribed region.⁴ In such cases, a circumscribed, spatially contiguous resection may not result in seizure freedom.^{8,9} There is a critical need to quantify the extent of the epileptogenic tissue and measure the impact of planned surgery to predict seizure outcomes more accurately.^{10,11}

Several studies have investigated both structural and functional networks in epilepsy,^{10–21} but there is a need for more studies that correlate the 2 types of networks, especially using iEEG.^{22–25} Given that structural connectivity (SC) constrains functional connectivity (FC), and FC modulates SC through plasticity mechanisms, these relationships may offer valuable insights into the underlying mechanisms.^{26,27} A recent study showed increased coupling between SC and iEEG-derived FC at seizure onset, revealing the structural substrate that supports seizure spread.²³ Other studies have also indicated that combining information from both SC and FC could improve the localization of seizure generators.^{9,25,28,29} Of interest, there is a lack of studies examining the relationship between the efficacy of epilepsy surgery and structure-function relationships. Surgical resection leads to structural changes in the brain to control abnormal function, so the structure-function relationships before and expected after surgery could be crucial factors in determining surgical outcomes.

Our primary research question is whether structure-function mapping helps determine the outcome of surgical resection for treatment-resistant focal epilepsy. We hypothesized that surgical resection would effectively control seizures when there is a strong coupling between brain structure and function. Our reasoning is that a stronger structure-function coupling would provide a more effective means of transmitting the structural changes in the epileptic network caused by surgery to the FC that is necessary for seizure expression. To test this hypothesis, we studied individuals with intractable epilepsy who underwent resective surgery after iEEG implantation. Initially, we quantified the structure-function coupling at the global iEEG network level. Next, we performed virtual surgeries retrospectively to estimate the effect of removing individual brain areas on the remaining network as a spatial map. This mapping enabled us to translate the global-network metric of structure-function coupling into a regional metric that aided in localization of epileptogenic tissues. Finally, we emphasize the importance of considering structure-function coupling measures in addition to other clinical attributes to accurately predict seizure outcomes after epilepsy surgery.

Methods

Patient Cohort

We retrospectively studied a patient cohort with drug-resistant focal epilepsy, recruited at the National Hospital for Neurology and Neurosurgery (NHNN), UK. The patients underwent MRI sequences and iEEG monitoring using either electrocorticography (ECOG) or stereotactic EEG (SEEG) based on the clinical need. The surgical planning for removing the seizure-onset zone in each case was made by mapping the eloquent brain function and considering the risk-benefit ratio of the resection. The patients were followed up for at least 12 months after surgery, and their seizure outcomes were evaluated using the International League Against Epilepsy (ILAE) classification of postoperative seizure outcome.³⁰ We included all patients with available iEEG and diffusion MRI data

from 2009 to 2014, along with the routine MRI scans, without any specific criteria for selection based on the laterality of the implantation or seizure-onset zone.

Standard Protocol Approvals, Registrations, and Patient Consents

The study was approved by the NHNN and Institute of Neurology Joint Research Ethics Committee. The data were analyzed with approval from the Newcastle University Ethics Committee (ref: 1804/2020). The ethics board determined that because this was a retrospective analysis of anonymized data, participant consent was not required or waived.

MRI and iEEG Data Acquisition

Preoperatively, each patient underwent an anatomical T1-weighted and diffusion-weighted MRI. After iEEG implantation, CT scans were obtained to localize electrode contacts, and T1-weighted MRI was acquired 3–12 months after surgery to outline the extent of resection.

The T1-weighted MRI was acquired on a 3T GE Signa HDx scanner with standard imaging gradients, with a maximum strength of 40 mT m^{-1} and slew rate $150 \text{ T m}^{-1} \text{ s}^{-1}$. Standard clinical sequences were performed, including a coronal 3-dimensional volumetric acquisition (matrix = $256 \times 256 \times 170$; resolution = $0.9375 \times 0.9375 \times 1.1 \text{ mm}$).

Diffusion-weighted MRI was acquired with a single-shot spin-echo planar imaging sequence using 52 noncollinear directions (b value = $1,200 \text{ mm}^2 \text{ s}^{-1}$, δ = 21 milliseconds, Δ = 29 milliseconds using full-gradient strength of 40 mT m^{-1} , echo time 73 milliseconds) and 60 contiguous 2.4 mm axial slices covering the brain, along with 6 nondiffusion weighted scans. The field of view was $24 \times 24 \text{ cm}$ and the acquisition matrix size was 96×96 (zero-filled to 128×128), resulting in a voxel size of $1.875 \times 1.875 \times 2.4 \text{ mm}$ and acquisition time of 25 minutes.

iEEG was sampled at 512 Hz or 1,024 Hz. Table 1 shows the type of implantation (ECOG/SEEG) and the number of implanted electrodes in each patient. We extracted 1-hour segments of awake interictal EEG data, at least 2 hours away from seizures, as identified by the clinical team and described previously.¹³

Data Preprocessing

We linearly registered the postoperative T1-weighted to preoperative T1-weighted MRI using the FSL-FLIRT algorithm. We manually drew a resection mask for every patient, ensuring high interrater agreement to identify surgically resected tissue.¹¹ We ran the FreeSurfer “recon-all” pipeline on preoperative T1-weighted MRI to generate gray and white matter surfaces.^{10,31}

Diffusion-weighted MRI was corrected for signal drift, eddy current, and movement artifacts using the FSL eddy_correct tool, and the b vectors were rotated using the FSL fdt-rotate-vecs tool.^{10,31} We applied generalized q-sampling imaging

reconstruction in DSI studio with a diffusion sampling length ratio of 1.25, followed by deterministic tractography.³² Tractography generated approximately 2 million tracts per person with tracking parameters configured as follows: Runge-Kutta method with step size 1 mm, whole-brain seeding, initial propagation direction set to all fiber orientations, minimum tract length 15 mm, maximum tract length 300 mm, and topology-informed pruning applied with 1 iteration to remove false connections. Linear registration was applied to transform the tracts generated in the diffusion space to the preoperative T1-weighted MRI space.

Following our previous study,¹³ we processed the iEEG data in 3 steps: (1) removing artifactual channels by visual inspection, (2) applying a common average reference to all remaining channels, and (3) filtering each channel with a notch filter at 50 and 100 Hz (infinite impulse response filter with Q factor = 50, fourth-order zero-phase lag) and bandpass filter (Butterworth fourth-order zero-phase lag) between 1 and 70 Hz. For frequency band-specific analysis, we separately filtered the interictal signals in 6 frequency bands—delta (1–4 Hz), theta (4–8 Hz), alpha (8–13 Hz), beta (13–30 Hz), gamma (30–80 Hz), and high gamma (80–150 Hz).

To delineate electrode contacts overlapping the tissue that was subsequently resected, we linearly registered the CT image to the presurgery T1-weighted MRI space and marked the electrode coordinates semiautomatically.¹³ We considered any electrode within 5 mm of the surgically resected tissue, as identified by the segmented postoperative MRI, as resected. Figure 1, A–G illustrates an overview of different imaging modalities.

Network Generation

We estimated the SC and FC between brain areas implanted by electrodes. The brain tissue underlying each electrode comprised the nodes of the network, so the number of network nodes equaled the number of implanted electrodes (excluding those affected by artifacts or outside the brain).

To estimate SC, we delineated the tracts intercepted by each electrode. We used the following atlas-agnostic steps to delineate these tracts from the whole-brain tractography data (Figure 1G). First, for each contact in the neocortical gray matter (pial) surface, we found the corresponding coordinate on the white matter surface. This step was not necessary for contacts in the white matter or deep brain structures (e.g., hippocampus). Second, we sampled all tracts that passed within a 2 mm spherical diameter and connected at least 2 electrodes. Third, we computed the total number of tracts between electrodes to measure SC. Because all network nodes have same spherical diameters, this connectivity metric can be considered equivalent to streamline density, as used in many other studies.³³ Figure 1, H–J illustrates the tracts between contacts and SC in 1 case. To verify the robustness of our results, we recomputed SC with an alternate diffusion metric that captures the average tract length between contacts and

Table 1 Demographic and Clinical Data

Variables	Groups		Significance
	Seizure-free	Not seizure-free	
Patients, n	15	24	
Sex (male/female), n	8/7	8/16	$\chi^2 = 0.81$ $p = 0.37$
Side of surgery (left/right), n	8/7	12/12	$\chi^2 = 0.02$ $p = 0.90$
Hippocampal sclerosis, n (%)	4 (26.7)	3 (12.5)	$\chi^2 = 0.48$ $p = 0.49$
Preoperative MRI (normal/abnormal), n	4/11	12/12	$\chi^2 = 1.22$ $p = 0.27$
History of FBTCS, n (%)	9 (60)	16 (66.7)	$\chi^2 = 0.01$ $p = 0.94$
History of status epilepticus, n (%)	4 (26.7)	5 (20.8)	$\chi^2 < 0.01$ $p = 0.98$
Electrode implantation type (ECOG/SEEG), n	4/11	7/17	$\chi^2 = 0.04$ $p = 0.84$
Surgery location (TLE/eTLE), n	10/5	12/12	$\chi^2 = 0.48$ $p = 0.49$
Partial resection of the seizure-onset zone, n (%)	5 (33.3)	16 (66.6)	$\chi^2 = 2.89$ $p = 0.09$
Unilateral seizure-onset zone, n (%)	13 (86.6)	24 (100)	$\chi^2 = 1.19$ $p = 0.28$
Unilateral iEEG implantation, n (%)	12 (80)	24 (100)	$\chi^2 = 2.76$ $p = 0.10$
Age at surgery, y, median \pm IQR	28.2 \pm 5.4	31.9 \pm 17.4	$d = 0.36$ $p = 0.46$
Age at epilepsy onset, y, median \pm IQR	10.0 \pm 9.5	13.5 \pm 11.5	$d = 0.69$ $p = 0.07$
Epilepsy duration, y, median \pm IQR	22.5 \pm 7.2	19.6 \pm 10.4	$d = 0.07$ $p = 0.57$
All ASMs before surgery, median \pm IQR	7 \pm 4	7 \pm 3	$d = 0.07$ $p = 0.87$
Total electrode contacts implanted, median \pm IQR	73 \pm 45	73 \pm 34	$d = 0.002$ $p = 0.97$

Abbreviations: χ^2 = chi-square test for categorical variables; d = Cohen d score for the effect size; p = 2-tailed Wilcoxon rank-sum test; ASM = anti-seizure medication; ECOG = electrocorticography; eTLE = extratemporal lobe epilepsy; FBTCS = focal to bilateral tonic-clonic seizures; iEEG = intracranial EEG; IQR = interquartile range; SEEG = stereo-EEG; TLE = temporal lobe epilepsy.

by varying the spherical diameter at each contact with different thresholds at 5 mm (eFigures 1 and 2, links.lww.com/WNL/D22).

We estimated FC between each electrode pair from the preprocessed, 1-hour interictal segments of iEEG filtered in broadband (1–70 Hz) and 6 frequency bands.¹³ We applied the Pearson correlation to 2-second sliding windows (without overlap) and averaged the correlation matrices over all

windows to obtain 1 FC network. Figure 1, K and L illustrates the FC network in 1 case, highlighting the structurally connected (direct) and structurally unconnected (indirect) functional connections.

eFigure 3 (links.lww.com/WNL/D22) illustrates the reproducibility of 2 widely reported findings in our network data³⁴: (1) significantly stronger mean FC between structurally connected node pairs compared with structurally unconnected node pairs and (2) decline in the strength of FC between structurally connected and unconnected node pairs in relation to Euclidean distance.

Structure-Function Coupling Analysis and Virtual Resection Approach

We modeled the relationship between structural and functional networks at the global iEEG network level resolution by computing Spearman's rank correlation between the connections present in both the SC and FC networks (Figure 2, A and B).

To investigate the localizing value of SC-FC coupling at a more fine-grained resolution, we performed virtual surgeries on brain networks (Figure 2, C–E). First, we removed a node and its corresponding connections in SC and FC. Second, we recomputed Spearman's rank correlation between SC and FC of the remaining network. Third, we obtained the difference between the SC-FC coupling before surgery and after node removal. This difference reflected the impact of removing that node on the SC-FC coupling of the remaining network.^{23,35} We repeated these steps by removing 1 node at a time, noting the changes in the SC-FC coupling each time, and expressing these changes as a z score in each patient's brain network to generate a spatial map (Figure 2F).

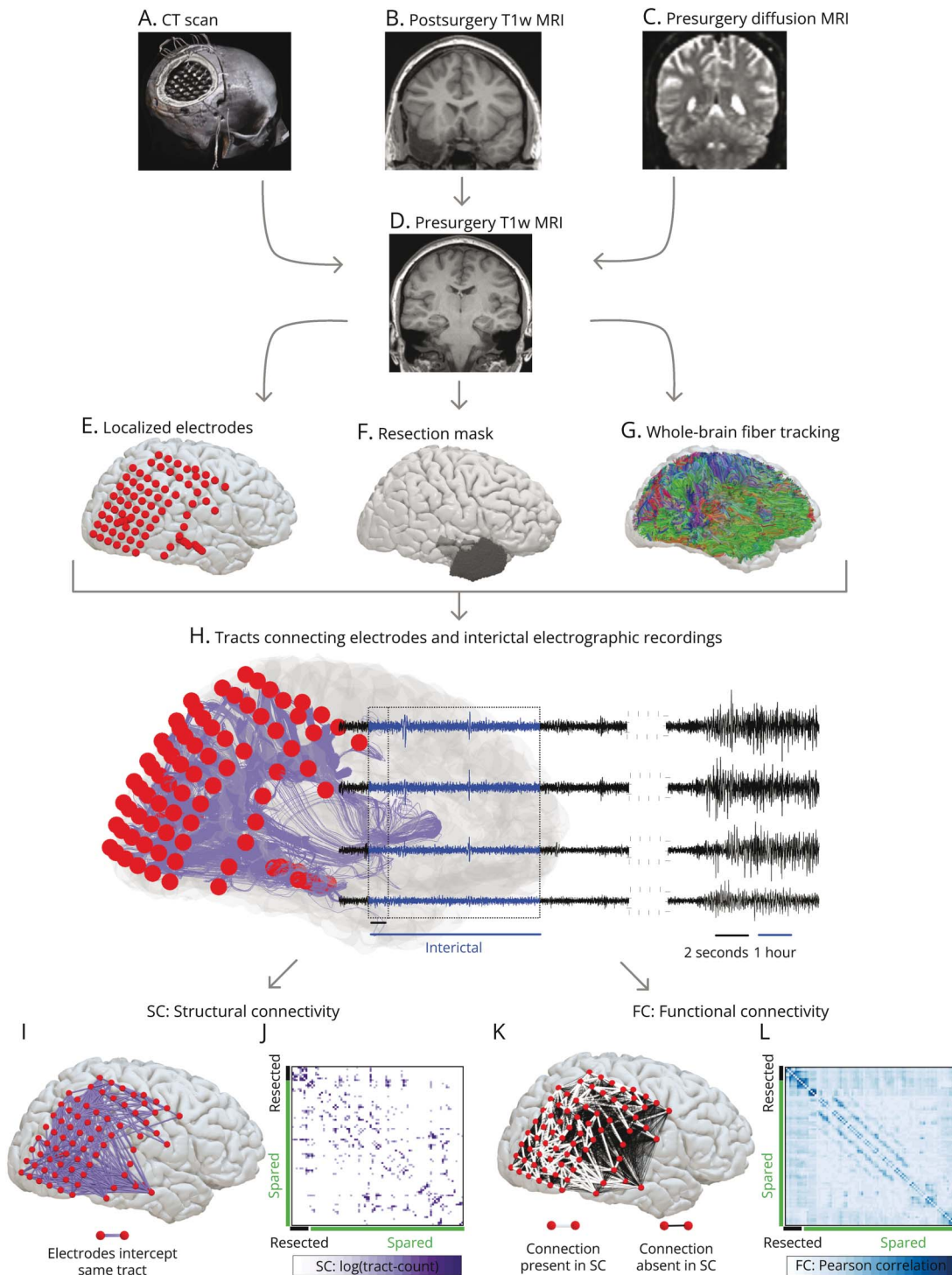
We also applied another variation of a virtual resection approach to ensure robustness.^{14,36} Instead of removing 1 node at a time, we removed all nodes deemed resected, as defined by the postoperative MRI, and compared the change in SC-FC coupling with changes due to random resection of the same number of nodes; eFigure 4 (links.lww.com/WNL/D22) describes this approach in detail.

Predictive Model Design

We used a support vector machine (SVM) to predict seizure freedom after surgery.^{10,37} The SVM inputs were 16 clinical features (Table 1) and 2 coupling features, with binary outcomes of seizure-free or not seizure-free. A linear kernel was used for interpretable feature weights. The data were split into training and testing sets using leave-one-out cross-validation, and the SVM was trained on the training set and evaluated on the test set to assess its performance.

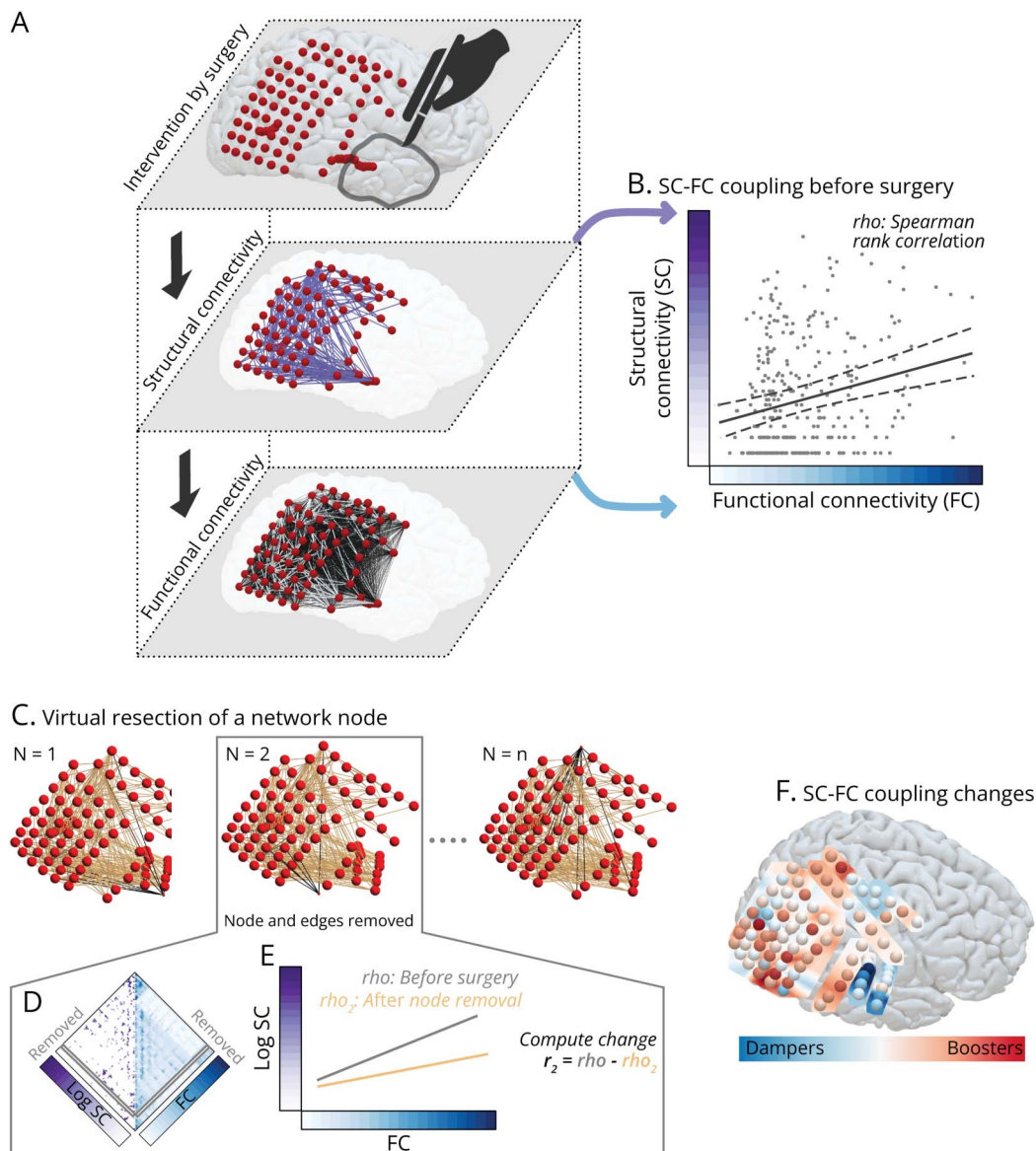
To evaluate the feature importance, we used a method called SVM recursive feature elimination. This approach involved starting with all 16 clinical features and 2 coupling measures as inputs for the SVM. The performance of the model was

Figure 1 Overview of Network Generation



Panels (A–D) show different modalities acquired for each patient. We aligned the CT scan in panel (A) to the presurgery T1w MRI in panel (D) to delineate the coordinates of implanted electrodes shown in panel (E). We registered the postsurgery T1w MRI in (B) with the presurgery T1w MRI scan in (A) to manually draw a resection mask in the presurgery T1w MRI space illustrated in panel (F). We performed the whole-brain fiber tracking on presurgery diffusion MRI in the native space (C) and then aligned the tracts to the presurgery T1-MRI space shown in panel (G). In panel (H), we combined electrode coordinates, tracts, and surgery information. The example case illustrated in the figure was not seizure-free after the surgery. From the whole-brain fiber tracts, we delineated the tracts connecting each electrode shown in purple. Each electrode (in red) records the electrophysiologic signals (in black) directly from the cortical tissues. We analyzed 1-hour interictal segments (in blue) at least 2 hours from seizures. By counting the number of tracts between each electrode, we constructed the structural connectivity. Panel (I) maps the binarized structural connectivity network for illustrating connections between electrodes. Panel (J) shows the weighted structural connectivity matrix with tract counts transformed on a log scale. Rows and columns of the connectivity matrix are the electrodes; spared electrodes labeled in green, and resected electrodes labeled in black. Panel (K) depicts the functional connectivity network derived from 2-second windows of 1-hour interictal iEEG recordings. Functional connections with underlying structural connections are shown in white, and the remaining structurally unconnected functional connections are shown in black. Panel (L) shows the weighted functional connectivity matrix with electrodes in rows and columns reordered as spared (green) and resected (black) contacts. iEEG = intracranial EEG; T1w = T1 weighted.

Figure 2 Virtual Resection Approach for Estimating Changes in Structure-Function Coupling

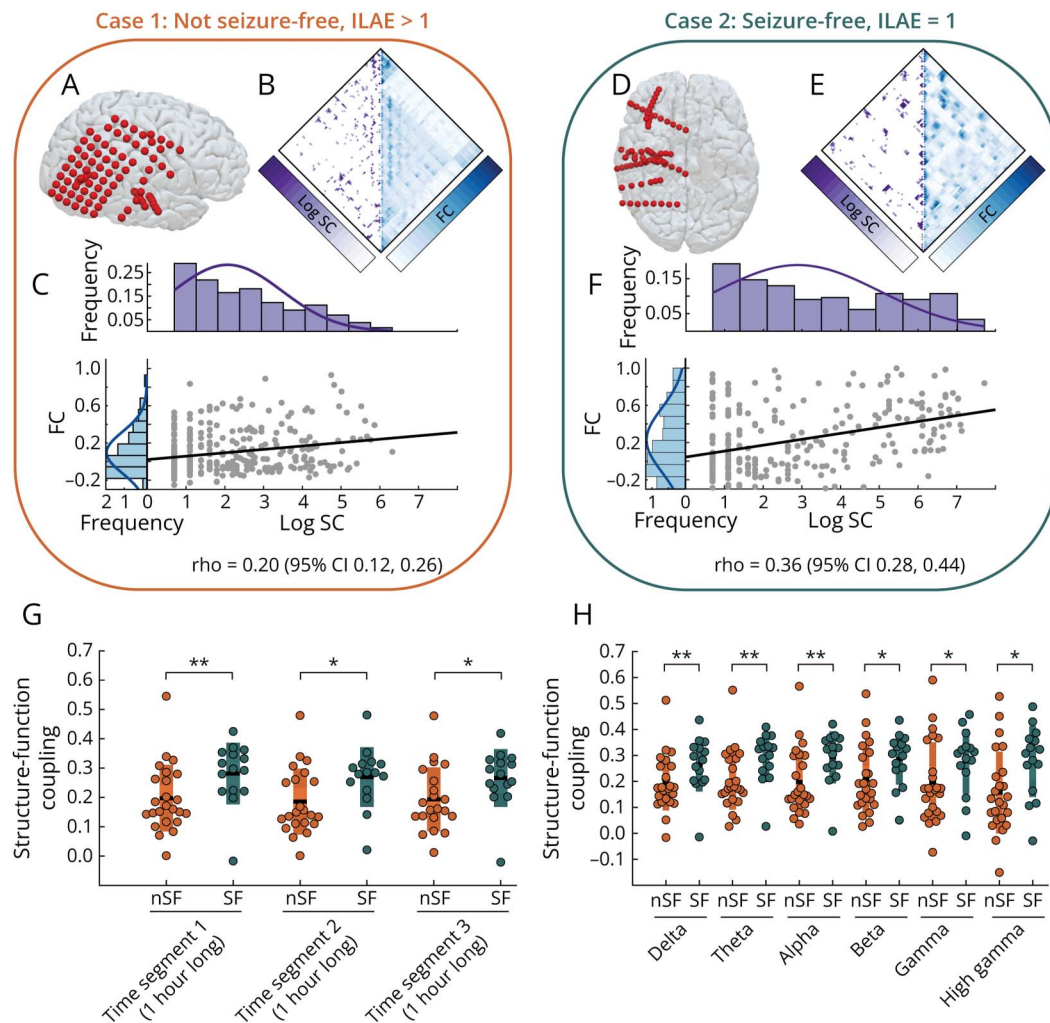


Panel (A) conceptualizes a common framework to study surgical intervention and its impact on the SC and FC networks as 3 interlinked layers. Resecting localized cortical tissue by surgery alters the brain anatomy and the underlying structural network. An assumption is that the structure and function are strongly interlinked, and alteration to the structure would change the function to control the abnormal functional dynamics associated with seizures. Panel (B) illustrates structure-function coupling modeled by Spearman's rank correlation as a measure to evaluate the strength of interlinking between structure and function in brain areas sampled by iEEG electrodes. Each point in the scatter plot represents a network connection. In panel (C-E), we estimated the impact of removing individual brain areas on the structure-function coupling by applying virtual resection of network nodes. Panel (C) illustrates the removal of a node (drawn smaller) and corresponding edges (in black). Removing a network node is equivalent to removing a row and a column from the structural and functional connectivity matrices in (D). In panel (E), we re-evaluated Spearman's rank correlation between the remaining connections of structure-function networks. We computed the change in coupling between networks after virtual resection and the original network with all nodes intact. Panel (F) maps the changes in SC-FC coupling. We detected that some cortical areas are coupling boosters (in red)—removing these nodes boosted the SC-FC coupling of the remaining network. Also, some other cortical areas are coupling dampers (in blue)—removing these nodes dampened the SC-FC coupling of the remaining network. Removing the red coupling boosters may improve the chance of seizure-free outcomes; however, these areas are scattered, indicating a distributed epileptogenic network. The illustrated case was not seizure-free after the surgery. FC = functional connectivity; iEEG = intracranial EEG; SC = structural connectivity.

measured using the area under the receiver operating characteristic curve (AUC), and the features were ranked based on their relative importance. The least important feature was then removed, and the SVM performance was re-evaluated with 1 less feature. This process was repeated until only 1 feature remained, leading to the identification of the most informative feature combination for predicting seizure outcomes in the patient cohort.

To address the potential impact of the small dataset size on the bias-variance trade-off, we conducted a stability analysis using nested cross-validation. In this method, 10% of the patients were set aside for testing, and the remaining patients underwent k -fold cross-validation (with $k = 5$) to train and evaluate the model. The entire analysis was then repeated 5,000 times to randomly hold out the test dataset. This allowed us to evaluate the consistency of the model's predictions by assessing the variability in predicted outcomes.

Figure 3 Structure-Function Coupling Is Significantly Higher in the SF Group Than in the nSF Group



Panels (A–C) illustrate example case 1 who was nSF after surgery: electrode coordinates in (A), SC and FC matrices in (B), and SC-FC coupling between structural and functional edges in (C). The histograms in (C) show the distribution of structural and functional edges in purple and blue, respectively. Panels (D–F) show equivalent plots for an individual who is SF after surgery. SF case 2 had a significantly higher (nonoverlapping 95% CI of p) SC-FC coupling than nSF person 1. Panel (G) illustrates the SC-FC coupling at the group level between SF (in teal) and nSF (in orange) individuals across 3 different interictal time segments of iEEG recordings. Those who were SF have a significantly higher structure-function coupling than those who were not. Statistical estimates: Segment 1: $p = 0.002$, $d = 0.76$, AUC = 0.78 (95% CI 0.62–0.93); segment 2: $p = 0.009$, $d = 0.77$, AUC = 0.73 (95% CI 0.56–0.90); and segment 3: $p = 0.008$, $d = 0.70$, AUC = 0.74 (95% CI 0.57–0.91). In panel (H), we evaluated the structure-function coupling between SF and nSF individuals across different frequency bands. Across all frequency bands, the structure-function coupling is significantly higher in those who are SF than in those who are not. Statistical estimates: delta (1–4 Hz): $p = 0.003$, $d = 0.68$, AUC = 0.76 (95% CI 0.60–0.92); theta (4–8 Hz): $p = 0.001$, $d = 0.83$, AUC = 0.79 (95% CI 0.64–0.95); alpha (8–13 Hz): $p = 0.003$, $d = 0.81$, AUC = 0.76 (95% CI 0.60–0.92); beta (13–30 Hz): $p = 0.015$, $d = 0.66$, AUC = 0.71 (95% CI 0.53–0.88); gamma (30–80 Hz): $p = 0.033$, $d = 0.56$, AUC = 0.68 (95% CI 0.5–0.86); and high gamma (80–150 Hz): $p = 0.01$, $d = 0.79$, AUC = 0.72 (95% CI 0.55–0.89). AUC = area under the receiver operating characteristic curve; FC = functional connectivity; iEEG = intracranial EEG; ILAE = International League Against Epilepsy; nSF = not seizure-free; SC = structural connectivity; SF = seizure-free.

Statistical Analysis

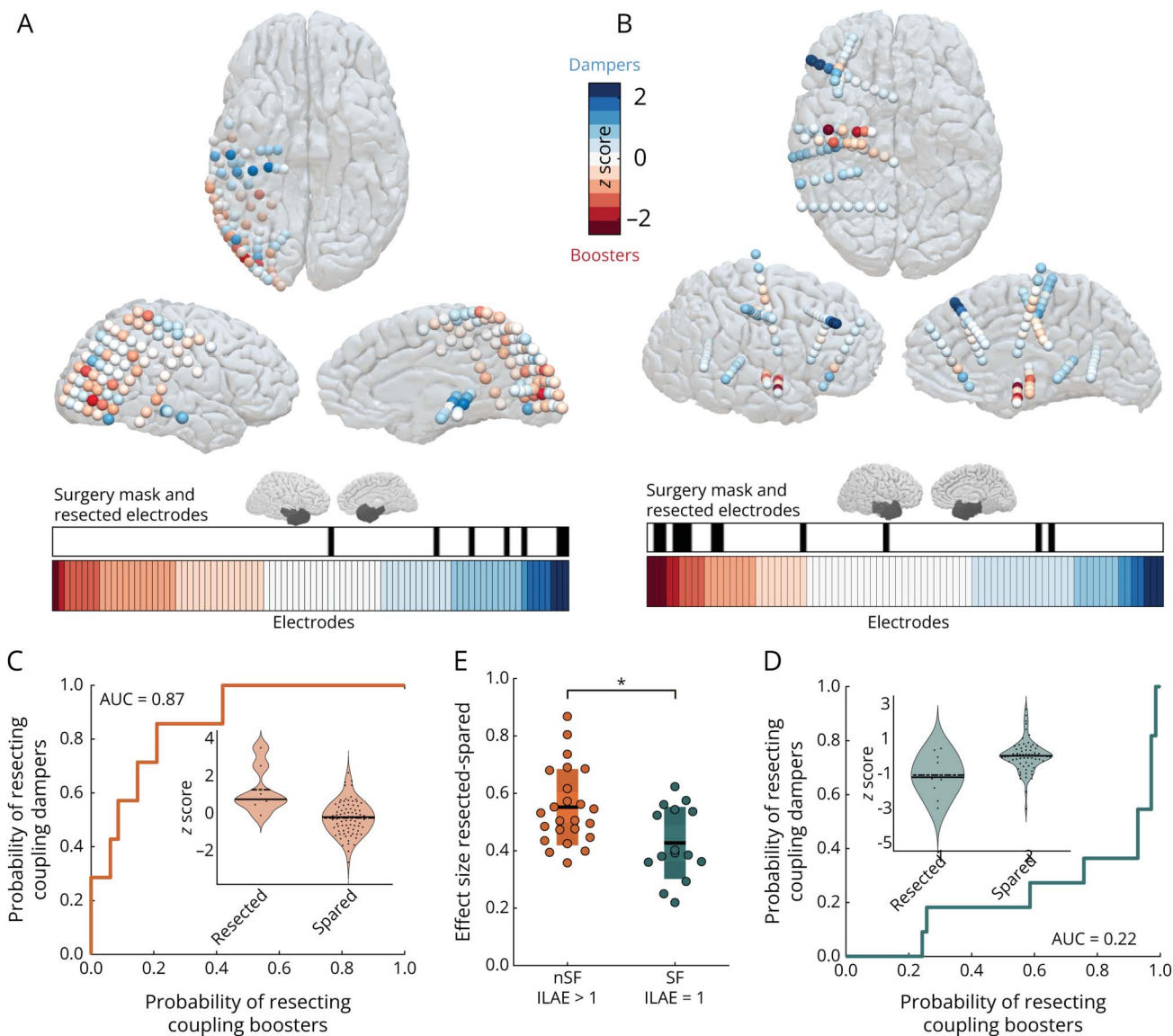
To model the coupling between structure and function, we performed robust estimation to obtain the regression line and calculated the nonparametric Spearman’s rank correlation. These approaches are less sensitive to the effect of outliers and appropriate when the normal distribution in data cannot be assumed. For testing the hypothesis that structure-function coupling is higher in seizure-free individuals compared with those who are not seizure-free, we applied a 1-tailed nonparametric Wilcoxon rank-sum test and calculated the effect size as Cohen’s d score and nonparametric effect size as AUC.

Results were considered significant for $p < 0.05$. To correct multiple comparisons, we applied Benjamini-Hochberg false discovery rate correction at a significance level of 5%. In machine learning analysis, we report the 95% CI of the AUC using a bias-corrected and accelerated percentile method from 10,000 bootstrap resamples with replacement.^{10,31}

Data Availability

All anonymized brain networks and electrode coordinates with resection indicators included in this study are available at <https://doi.org/10.5281/zenodo.8246573>.

Figure 4 Surgeries in Not Seizure-Free Individuals Overlap With Coupling Dampers, Whereas in Those Who Are Seizure-Free, Surgery Overlaps With Coupling Boosters



Panel (A) plots the iEEG electrodes as coupling boosters and dampers for case 1 (not seizure-free). The surgery mask in the sagittal view shows the location of the resected tissue. The color bar plotted horizontally shows the implanted electrodes in case 1 sorted by coupling booster-damper metric, and the binary plot in black highlights the resected electrodes. Panel (B) shows the equivalent contrasting plots for case 2 (seizure-free). Panel (C) quantifies the overlap between surgery and coupling booster-damper metric of electrodes for case 1 by computing the AUC. Panel (D) shows the equivalent plot for case 2. AUC is a nonparametric effect size to discriminate between resected and spared tissues. This effect size is a patient-specific measure that quantifies the probability of resecting coupling dampers for $0.5 < \text{AUC} \leq 1$, resecting coupling boosters for $0 < \text{AUC} < 0.5$, and chance-level probability of resecting coupling boosters or dampers for $\text{AUC} = 0.5$. The violin plots in the inset show coupling booster-damper data points for each electrode categorized as resected or spared. Panel (E) shows that the effect size between resected and spared tissues (AUC) is significantly higher in individuals who are not seizure-free than in those who are seizure-free ($p = 0.007$, $d = 0.96$ [95% CI 0.34–1.56]). AUC = area under the receiver operating characteristic curve; iEEG = intracranial EEG.

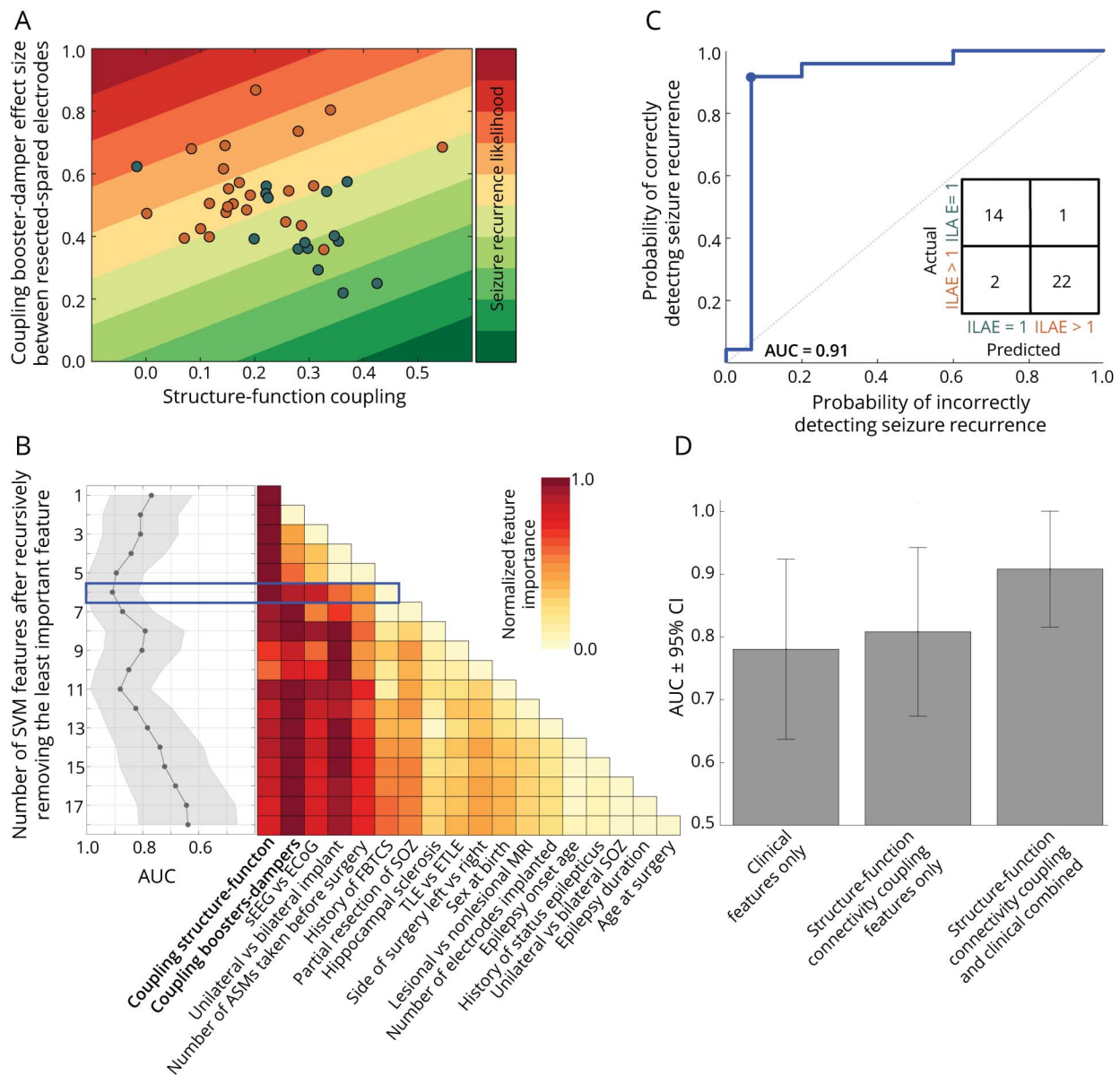
Results

Participants

We retrospectively analyzed 39 patients with drug-resistant focal epilepsy. Table 1 provides a summary of the clinical and demographic characteristics of the study participants. A more comprehensive view is available in eTable 1 (links.lww.com/WNL/D23). During the study, 28 patients underwent iEEG monitoring using ECOG, and 11 received SEEG. The

surgical resections were performed in various brain regions, including the temporal lobe ($n = 22$), frontal lobe ($n = 12$), parietal lobe ($n = 3$), and occipital lobe ($n = 2$). We found that 15 patients were seizure-free (ILAE 1), and 24 had seizure recurrence (ILAE 2–5). Demographic information and clinical attributes, such as the type of electrode implantation (SEEG vs ECOG) or the number of implanted electrode contacts, did not differentiate between seizure outcomes.

Figure 5 Importance of the Structure-Function Coupling in Seizure Outcome Prediction



Panel (A) shows a scatter plot of the relationship between the structure-function coupling of brain networks before surgery and the discrimination between resected and spared tissue using the coupling booster-damper metric. The 2-dimensional plane is color coded to indicate the likelihood of seizure recurrence. The dots represent individual patients, with those who are seizure-free in teal and those who are not seizure-free in orange. The 2 coupling measures are not correlated but together provide complementary information that distinguishes those who are seizure-free from those who are not. (B) The 2 coupling measures were combined with 16 clinical features in a linear SVM model to predict seizure outcomes after surgery. The feature importance was evaluated through a recursive removal process, and the model performance was noted after each iteration. The color plot shows the normalized feature importance after each round, and the graph on the left shows the AUC \pm 95% CI. The blue box highlights the iteration where AUC was maximized. Panel (C) shows the ROC curve at iteration 6 (highlighted in blue), with the confusion matrix in the inset. The predictive performance estimates are as follows: Number of features = 6, AUC = 0.91 [95% CI 0.82–1.0], with accuracy = 92%, sensitivity = 93%, and specificity = 91% at the optimal operating point (represented by the blue dot on the ROC curve). Panel (D) compares the efficacy of different models in predicting surgical outcomes based on inputs consisting of only clinical features (AUC 0.78 [95% CI 0.64–0.92]), only connectivity coupling features (AUC 0.81 [95% CI 0.67–0.94]), and a combination of both (AUC 0.91 [95% CI 0.82–1.0]). The results show that combining connectivity coupling measures with clinical variables leads to improved prediction of seizure outcomes. ASMs = antiseizure medications; AUC = area under the ROC curve; ECOG = electrocorticography; ETL = extratemporal lobe epilepsy; FBTCS = focal to bilateral tonic-clonic seizures; ILAE = International League Against Epilepsy; ROC = receiver operating characteristic; sEEG = stereo-EEG; SOZ = seizure-onset zone; SVM = support vector machine; TLE = temporal lobe epilepsy.

Impact of SC-FC Coupling on Seizure Outcomes After Epilepsy Surgery

Brain areas implanted by iEEG electrodes had a stronger SC-FC coupling in seizure-free patients than those who were not seizure-free. Figure 3, A–F illustrates iEEG

implantations in 2 cases: not seizure-free case 1 and seizure-free case 2. At the location of iEEG implantation, Figure 3, B and E maps patient-specific SC and FC measured from brain regions underlying each electrode. We found that seizure-free case 2 had a higher SC-FC coupling ($\rho = 0.36$ [95% CI

0.28–0.44]) than not seizure-free case 1 ($\rho = 0.20$ [95% CI 0.12–0.26]).

Across the entire cohort, we detected a significantly higher SC-FC coupling in the seizure-free group than the not seizure-free group ($p = 0.002$, $d = 0.76$, AUC = 0.78 [95% CI 0.62–0.93]), regardless of the choice of interictal time segments to estimate FC (Figure 3G). We did not find a specific frequency band driving the significantly higher SC-FC coupling in seizure-free individuals; rather, it was consistent across frequency bands (Figure 3H).

eFigures 1 and 2 (links.lww.com/WNL/D22) illustrate the consistency of our findings for variations in SC measurements estimated from the alternate diffusion metric and region size. Controlling for spatial biases,¹³ eFigure 5 demonstrates that SC-FC coupling explains the association with surgical outcomes more strongly than Euclidian distance. eFigure 6 shows the effect of implantation (ECOG vs SEEG) and alternate grouping of ILAE outcomes on SC-FC coupling. eFigures 7 and 8 show the consistency of our findings with alternate choices of iEEG rereferencing techniques. eFigure 9 shows that the contacts in the gray matter primarily drive our results; however, removing the contacts in the white matter led to a drop in the effect size.

Identifying Epileptogenic Tissues by Coupling Boosters

The virtual resection approach enabled us to quantify the impact of removing a specific brain area on SC-FC coupling. These coupling changes are presented as spatial maps at the resolution of individual brain areas underlying iEEG contacts (Figure 4, A and B). Red contacts with lower negative z scores are coupling boosters—removing these contacts boosts the coupling of the expected remaining network. Blue contacts with higher positive z scores are coupling dampers—removing these contacts dampens the coupling of the expected remaining network. The lower horizontal panel in Figure 4, A and B plots the electrode contacts sorted by SC-FC coupling changes. The electrode contacts marked in black in the panel above the color bar indicate the resected contacts. We found that surgery overlapped more with coupling dampers in patients who were not seizure-free, whereas in those who were seizure-free, surgery overlapped more with coupling boosters. Thus, regions identified as coupling boosters can help localize epileptogenic tissues.

With each electrode characterized as a coupling booster or damper, we computed a nonparametric effect size (AUC), identical to distinguishability statistics,¹³ to distinguish between resected and spared contacts. Figure 4, C and D illustrates the discrimination between resected and spared electrodes in 2 cases, and Figure 4E plots the effect size between seizure-free and not seizure-free groups. The probability of resecting coupling dampers in individuals who are not seizure-free is significantly higher than the probability of resecting coupling boosters in those who are seizure-free ($p = 0.007$, $d = 0.96$ [95% CI 0.34–1.56], AUC = 0.73 [95% CI 0.58–0.89]). Thus,

discrimination between resected and spared contacts characterized as coupling boosters and dampers is an important metric to determine seizure outcomes.

We verified the consistency of our findings with a different virtual resection strategy in eFigure 4 (links.lww.com/WNL/D22) and an MRI-derived expected postsurgery structural network, as in our previous studies,^{10,11} in eFigure 10.

Predicting Seizure Outcomes With Connectivity Coupling and Clinical Variables

We combined the SC-FC coupling measures from both the global iEEG network and individual brain areas as bivariate features. Figure 5A shows each patient on a 2-dimensional plane defined by these 2 coupling measures, and linear decision boundaries are drawn to map the likelihood of seizure recurrence. The 2 coupling measures were not correlated ($r = -0.21$, $p = 0.19$), and using a bivariate SVM model to combine them resulted in the discrimination of seizure-free and not seizure-free individuals with an AUC of 0.81 (95% CI 0.67–0.94). eFigure 11 (links.lww.com/WNL/D22) shows that the SC-FC coupling measures are not driven by a specific epilepsy subtype.

Next, we used the 2 coupling measures and the 16 clinical features listed in Table 1 to predict seizure outcomes. The linear SVM model was used with the leave-one-out cross-validation technique to predict seizure recurrence, and recursive feature elimination was applied to assess feature importance. Figure 5B shows the process of recursive feature elimination, with each feature ranked based on its relative importance (color coded in red). The highest AUC value was 0.91 (95% CI 0.82–1.0) when the SVM model combined the 2 connectivity coupling measures (the most important features) with 4 clinical variables: the type of electrode implantation, laterality of iEEG implantation, number of antiseizure medications taken before surgery, and history of focal to bilateral tonic-clonic seizures (Figure 5C). This combination of factors was found to best capture the variability in the data that predict surgical outcomes.

To evaluate the benefits of combining connectivity coupling measures with clinical variables in predicting surgical outcomes, we re-evaluated our analysis by using only the 16 clinical features listed in Table 1 and excluding the coupling measures. The results showed that using only the clinical variables resulted in an AUC of 0.78 (95% CI 0.64–0.92) (Figure 5D). Without the coupling measures, the 5 most important factors in determining surgical outcomes were partial resection of the seizure-onset zone, laterality of the iEEG implantation, lesional vs nonlesional MRI, age at epilepsy onset, and number of electrodes implanted (eFigure 12, links.lww.com/WNL/D22). Our findings suggest that combining the connectivity coupling measures with clinical variables enhances the prediction of seizure outcomes, with an accuracy of 92%, sensitivity of 93%, and specificity of 91%, compared with relying solely on clinical variables.

To verify the accuracy of our predictions, we used a nested cross-validation approach that included a 10% hold-out data and an internal 5-fold cross-validation. eFigure 13 (links.lww.com/WNL/D22) provides more information about this method and shows that it produced similar results to our original analysis, with an AUC of 0.90 and visualizations of the variability in predicted outcomes for individual patients.

Classification of Evidence

This is a Class IV retrospective case series showing that structure-function mapping may help determine outcomes from surgical resection for treatment-resistant focal epilepsy.

Discussion

We analyzed the relationship between structure and function in patients with drug-resistant focal epilepsy using a combination of diffusion-weighted MRI and iEEG. We found that a stronger relationship between structure and function was associated with seizure-free outcomes after surgery. Our findings suggest that patients are more likely to achieve seizure freedom if the relationship between structure and function becomes stronger after surgery. By identifying individual brain areas underlying each iEEG contact as coupling boosters or dampers, we demonstrate that the relationship between structure and function can be analyzed at a higher spatial resolution. This information could be useful during iEEG monitoring to identify the location of epileptogenic tissue more accurately. Our study demonstrates that by quantifying the relationship between structure and function in drug-resistant epilepsy, it is possible to make more accurate predictions about seizure outcomes. When used in conjunction with routine clinical variables, this information can help identify patients who are less likely to achieve seizure freedom through planned resection.

A strong coupling between the structural and functional networks of the brain is considered a hallmark of a healthy brain, as demonstrated in numerous studies.^{34,38,39} By contrast, a drop in SC-FC coupling has been linked to epilepsy and longer disease duration.⁴⁰ Healthy patients have been shown to have moderate to tight coupling, with levels as high as 0.9 ± 0.1 at the group level and 0.55 ± 0.1 at the individual patient level.³⁸ In people with epilepsy, reduced SC-FC coupling has been observed, particularly in those with longer disease duration.⁴⁰ We found that individuals with drug-resistant focal epilepsy who are not seizure-free after surgery have weaker structure-function coupling compared with those who are seizure-free. Our study provides evidence that the strength of structure-function connectivity coupling plays a significant role in determining the success of epilepsy surgery. Individuals with a stronger structure-function coupling before surgery and who undergo surgical resections that increase the structure-function coupling of the remaining network are more likely to achieve seizure-free outcomes. Our findings align with previous studies that have shown the importance of structure-function connectivity coupling in maintaining a

healthy brain and highlight the potential for using this metric to optimize surgical interventions for epilepsy.

Our findings have significant clinical implications. First, our results can aid in identifying the focality of iEEG implantation.⁴¹ We generated patient-specific maps of the relationship between structural and functional brain networks, which classified the brain tissue under each iEEG contact as either a coupling booster or damper. Epileptogenic tissues (i.e., resections in seizure-free patients) were identified by the presence of coupling boosters. Thus, if coupling boosters are widespread, the epileptogenic tissue is dispersed, whereas if they are localized to a specific area, the epileptogenic tissue is focal. Second, our results can help predict seizure outcomes after surgery. Even with accurate iEEG localization, a patient may not be seizure-free if surgery cannot remove the entire epileptogenic tissue. Our study showed that determining the difference in coupling boosters and dampers between tissues that were removed and those that were preserved can predict seizure outcomes. Furthermore, at the iEEG network level, patients with reduced structural-functional coupling had a propensity toward seizure recurrence. Third, our analysis can aid in developing alternative surgical plans. The spatial maps quantifying the focality of iEEG implantation and predicting surgical outcomes for individual patients can guide treatment strategies prospectively. For example, a patient with a diffuse iEEG focus may be a better candidate for palliative therapies by neuromodulation.

Other studies have also made substantial progress in addressing these clinical challenges, leading to the development of quantitative measures such as node strength, seizure likelihood,^{14,36} brain network ictogenicity,²¹ neural fragility,⁴² and epileptogenicity index,⁴³ among others.^{9,28,29} However, despite surgical resection being a structural procedure to control function, most previous works overlooked the structure-function relationships of brain areas implanted by iEEG electrodes.^{23,44,45} Our study adds to this growing body of literature and closes a key gap in the field by proposing novel methods to combine iEEG and structural brain imaging for guiding epilepsy surgeries.

What is the added value in identifying structure-function relationships during presurgical workup over other measures already in clinical practice? Although some clinical variables such as a history of focal to bilateral tonic-clonic seizures are indicators of poor seizure outcomes, most studies report inconsistent findings; features found predictive of seizure outcomes in some studies are not predictive in others. A comprehensive analysis combined 27 clinical variables on a mixed cohort of people with temporal and extratemporal epilepsy to estimate the probability of seizure freedom.³⁷ Another study incorporated some of these variables on nomograms to evaluate the risk of poor surgical outcomes.⁴⁶ Our recent work benchmarked noninvasive surgical outcome measures against 13 clinical variables,¹⁰ which we also incorporate in this study to demonstrate the added value of new measures over routine clinical variables. We envision combining

these multimodal measures with unimodal measures from structural or functional imaging modalities and presurgical clinical data into a software tool⁴¹ for identifying individuals who are less likely to achieve seizure freedom.

Our study has limitations and important caveats that future studies should address. First, we could not directly perform a case-control analysis to compare the structure-function coupling between controls and epilepsy cases. People without epilepsy rarely undergo iEEG implantations, and it is difficult to estimate the strength of the structure-function coupling in a healthy population in areas where patients had iEEG implantations. However, future studies can leverage our recently proposed normative iEEG atlas as a promising alternative to circumvent the challenges associated with case-control analysis with iEEG data.^{47,48} Second, our analysis does not focus on reducing the invasiveness of iEEG. iEEG is among the most invasive diagnostic tools and should be used sparingly on carefully selected individuals who are highly likely to benefit from undergoing iEEG-related surgical procedures. Future studies could expand our analysis to a multilayer framework for making iEEG minimally invasive, including the development of robust methods for EMG artifact rejection,⁴⁹ or replacing it with complementary noninvasive modalities (e.g., fMRI, MEG, or high-density scalp EEG). Third, our analysis does not investigate the actual postsurgery networks, and the virtual surgery approach does not account for the second- or higher-order connectivity between nodes. Estimating the expected remaining network follows our previous approaches,^{10,11} designed for future prospective applications for any intended surgery. Nonetheless, validation on actual postsurgery data is important, and it can highlight the mechanisms of network changes due to surgery and its relation to outcomes.^{10,11} Fourth, our study dataset is limited in size and sourced from only 1 epilepsy center. Despite conducting stability analysis and various cross-validation techniques, surgical practices may differ across other epilepsy centers.⁵⁰ This study serves as a foundational step toward future multicenter research with a larger dataset. Finally, our analysis incorporated only the interictal/seizure-free epochs of iEEG data, which could be both a strength and a weakness. Many studies reported remarkable state changes in the preictal and ictal epochs that we do not analyze in this study.²³ However, a major strength in making predictions from seizure-free epochs is the reduction in time and injury risk associated with eliciting multiple seizures during iEEG monitoring.

In conclusion, we have shown that SC-FC coupling is an important measure that is related to seizure freedom after surgery. Structural alteration by surgery is more likely to control the abnormal functional dynamics associated with seizures when the coupling between structure and function is high. We suggest that mapping the impact of coupling changes at the resolution of individual brain areas can better evaluate surgical outcomes and create choices for alternative resection strategies, thus assisting the planning of epilepsy surgeries.

Acknowledgment

The authors acknowledge support from the UK Epilepsy Society. This work was supported by University College London Hospitals Comprehensive Biomedical Research Centre, which receives a proportion of funding from the UK Department of Health's National Institute for Health Research Centres funding scheme. The authors acknowledge the facilities and scientific and technical assistance of the National Imaging Facility, a National Collaborative Research Infrastructure Strategy (NCRIS) capability, at the Centre for Microscopy, Characterisation, and Analysis, the University of Western Australia.

Study Funding

This work was supported by the National Institute of Neurological Disorders and Stroke (R01NS116504), American Epilepsy Society (953257), Wellcome Trust WT 218380 (105617/Z/14/Z and 210109/Z/18/Z), UKRI Future Leaders Fellowship (MR/T04294X/1, MR/V026569/1), and MRC (G0802012, MR/M00841X/1).

Disclosure

N. Sinha acknowledges funding from the National Institute of Neurological Disorders and Stroke (R01NS116504) and American Epilepsy Society (953257). P.N. Taylor was supported by the Wellcome Trust (105617/Z/14/Z and 210109/Z/18/Z) and UKRI Future Leaders Fellowship (MR/T04294X/1). Y. Wang was supported by the Wellcome Trust (208940/Z/17/Z) and UKRI Future Leaders Fellowship (MR/V026569/1). K.A. Davis acknowledges funding from the National Institute of Neurological Disorders and Stroke (R01NS116504). J.S. Duncan and S.B. Vos were funded by the UCLH NIHR BRC and Wellcome Trust WT 218380. Scan acquisition and G.P. Winston were supported by the MRC (G0802012, MR/M00841X/1). All other authors report no disclosures relevant to the manuscript. Go to Neurology.org/N for full disclosures.

Publication History

Previously published at arXiv doi: 10.48550/arXiv.2204.08086. Submitted and externally peer reviewed. Received by *Neurology* July 24, 2022. Accepted in final form June 2, 2023. The handling editor was Associate Editor Barbara Jobst, MD, PhD, FAAN.

Appendix Authors

Name	Location	Contribution
Nishant Sinha, PhD	Department of Neurology, Penn Epilepsy Center, Perelman School of Medicine, and Center for Neuroengineering and Therapeutics, University of Pennsylvania, Philadelphia	Major role in the acquisition of data; drafting/revision of the manuscript for content, including medical writing for content; study concept or design; and analysis or interpretation of data
John S. Duncan, FRCP, FMedSci	Department of Epilepsy, UCL Queen Square Institute of Neurology, London; MRI Unit, Chalfont Centre for Epilepsy, Bucks, United Kingdom	Drafting/revision of the manuscript for content, including medical writing for content, and major role in the acquisition of data

Appendix (continued)

Name	Location	Contribution
Beate Diehl, PhD	Department of Epilepsy, UCL Queen Square Institute of Neurology, London, United Kingdom	Major role in the acquisition of data
Fahmida A. Chowdhury, PhD	Department of Epilepsy, UCL Queen Square Institute of Neurology, London, United Kingdom	Major role in the acquisition of data
Jane de Tisi, BA	Department of Epilepsy, UCL Queen Square Institute of Neurology, London, United Kingdom	Major role in the acquisition of data
Anna Miserocchi, FRCS (SN)	Department of Epilepsy, UCL Queen Square Institute of Neurology, London, United Kingdom	Major role in the acquisition of data
Andrew William McEvoy, FRCS (SN)	Department of Epilepsy, UCL Queen Square Institute of Neurology, London, United Kingdom	Major role in the acquisition of data
Kathryn A. Davis, MD, MSCE	Department of Neurology, Penn Epilepsy Center, Perelman School of Medicine, and Center for Neuroengineering and Therapeutics, University of Pennsylvania, Philadelphia	Drafting/revision of the manuscript for content, including medical writing for content
Sjoerd B. Vos, PhD	UCL Centre for Medical Image Computing; Neuroradiological Academic Unit, UCL Queen Square Institute of Neurology, London, United Kingdom; Centre for Microscopy, Characterisation, and Analysis, The University of Western Australia, Nedlands	Drafting/revision of the manuscript for content, including medical writing for content, and major role in the acquisition of data
Gavin P. Winston, BM BCh, PhD, FRCP	Department of Epilepsy, UCL Queen Square Institute of Neurology, London; MRI Unit, Chalfont Centre for Epilepsy, Bucks, United Kingdom; Division of Neurology, Department of Medicine, Queen's University, Kingston, Canada	Drafting/revision of the manuscript for content, including medical writing for content, and major role in the acquisition of data
Yujiang Wang, PhD	Translational and Clinical Research Institute, Faculty of Medical Sciences, and Computational Neuroscience, Neurology, and Psychiatry Lab, ICOS Group, School of Computing, Newcastle University; Department of Epilepsy, UCL Queen Square Institute of Neurology, London, United Kingdom	Major role in the acquisition of data; drafting/revision of the manuscript for content
Peter Neal Taylor, PhD	Translational and Clinical Research Institute, Faculty of Medical Sciences, and Computational Neuroscience, Neurology, and Psychiatry Lab, ICOS Group, School of Computing, Newcastle University, United Kingdom; Department of Epilepsy, UCL Queen Square Institute of Neurology, London, United Kingdom	Drafting/revision of the manuscript for content, including medical writing for content; study concept or design; major role in the acquisition of data; and analysis or interpretation of data

References

- Zijlmans M, Zweiphenning W, van Klink N. Changing concepts in presurgical assessment for epilepsy surgery. *Nat Rev Neurol*. 2019;15(10):594-606. doi:10.1038/s41582-019-0224-y
- Duncan JS, Winston GP, Koeppe MJ, Ourselin S. Brain imaging in the assessment for epilepsy surgery. *Lancet Neurol*. 2016;15(4):420-433. doi:10.1016/s1474-4422(15)00383-x
- Jobst BC, Cascino GD. Resective epilepsy surgery for drug-resistant focal epilepsy: a review. *JAMA*. 2015;313(3):285. doi:10.1001/jama.2014.17426
- Rosenow F, Lüders H. Presurgical evaluation of epilepsy. *Brain*. 2001;124(9):1683-1700. doi:10.1093/brain/124.9.1683
- Bartolomei F, Lagarde S, Wendling F, et al. Defining epileptogenic networks: Contribution of SEEG and signal analysis. *Epilepsia*. 2017;58(7):1131-1147. doi:10.1111/epi.13791
- Jehi L. The epileptogenic zone: concept and definition. *Epilepsy Curr*. 2018;18(1):12-16. doi:10.5698/1535-7597.18.1.12
- Kramer MA, Cash SS. Epilepsy as a disorder of cortical network organization. *Neuroscientist*. 2012;18(4):360-372. doi:10.1177/1073858411422754
- Keller SS, Glenn GR, Weber B, et al. Preoperative automated fibre quantification predicts postoperative seizure outcome in temporal lobe epilepsy. *Brain*. 2016;140(1):68-82. doi:10.1093/brain/aww280
- Besson P, Bandt SK, Proix T, et al. Anatomic consistencies across epilepsies: a stereotactic-EEG informed high-resolution structural connectivity study. *Brain*. 2017;140(10):2639-2652. doi:10.1093/brain/awx181
- Sinha N, Wang Y, Moreira da Silva N, et al. Structural brain network abnormalities and the probability of seizure recurrence after epilepsy surgery. *Neurology*. 2021;96(5):e758-e771. doi:10.1212/WNL.00000000000011315
- Taylor PN, Sinha N, Wang Y, et al. The impact of epilepsy surgery on the structural connectome and its relation to outcome. *Neuroimage Clin*. 2018;18:202-214. doi:10.1016/j.nicl.2018.01.028
- Sinha N, Peterzell N, Schroeder GM, et al. Focal to bilateral tonic-clonic seizures are associated with widespread network abnormality in temporal lobe epilepsy. *Epilepsia*. 2021;62(3):729-741. doi:10.1111/epi.16819
- Wang Y, Sinha N, Schroeder GM, et al. Interictal intracranial electroencephalography for predicting surgical success: the importance of space and time. *Epilepsia*. 2020;61(7):1417-1426. doi:10.1111/epi.16580
- Sinha N, Dauwels J, Kaiser M, et al. Predicting neurosurgical outcomes in focal epilepsy patients using computational modelling. *Brain*. 2017;140(2):319-332. doi:10.1093/brain/aww299
- Munsell BC, Gleichgerrcht E, Hofesmann E, et al. Personalized connectome fingerprints: their importance in cognition from childhood to adult years. *Neuroimage*. 2020;221:117122. doi:10.1016/j.neuroimage.2020.117122
- Bonilha L, Jensen JH, Baker N, et al. The brain connectome as a personalized biomarker of seizure outcomes after temporal lobectomy. *Neurology*. 2015;84(18):1846-1853. doi:10.1212/wnl.0000000000001548
- Englot DJ, D'Haese PF, Konrad PE, et al. Functional connectivity disturbances of the ascending reticular activating system in temporal lobe epilepsy. *J Neurol Neurosurg Psychiatry*. 2017;88(11):925-932. doi:10.1136/jnnp-2017-315732
- Morgan VL, Rogers BP, González HEJ, Goodale SE, Englot DJ. Characterization of postsurgical functional connectivity changes in temporal lobe epilepsy. *J Neurosurg*. 2020;133(2):392-402. doi:10.3171/2019.3.jns.19350
- Goodale SE, González HEJ, Johnson GW, et al. Resting-state SEEG may help localize epileptogenic brain regions. *Neurosurgery*. 2020;86(6):792-801. doi:10.1093/neuros/nyz351
- Lagarde S, Roehri N, Lambert I, et al. Interictal stereotactic-EEG functional connectivity in refractory focal epilepsies. *Brain*. 2018;141(10):2966-2980. doi:10.1093/brain/awy214
- Goodfellow M, Rummel C, Abela E, Richardson MP, Schindler K, Terry JR. Estimation of brain network ictogenicity predicts outcome from epilepsy surgery. *Sci Rep*. 2016;6(1):29215. doi:10.1038/srep29215
- Ashourvan A, Shah P, Pines A, et al. Pairwise maximum entropy model explains the role of white matter structure in shaping emergent co-activation states. *Commun Biol*. 2021;4(1):210. doi:10.1038/s42003-021-01700-6
- Shah P, Ashourvan A, Mikhail F, et al. Characterizing the role of the structural connectome in seizure dynamics. *Brain*. 2019;142(7):1955-1972. doi:10.1093/brain/awz125
- Carr SJA, Gershon A, Shafabadi N, Lhatoo SD, Tatsuoka C, Sahoo SS. An integrative approach to study structural and functional network connectivity in epilepsy using imaging and signal data. *Front Integr Neurosci*. 2020;14:491403. doi:10.3389/fnint.2020.491403
- Johnson GW, Doss DJ, Morgan VL, et al. The interictal suppression hypothesis in focal epilepsy: network-level supporting evidence. *Brain*. 2023;146(7):2828-2845. doi:10.1093/brain/awad016
- Chu CJ, Tanaka N, Diaz J, et al. EEG functional connectivity is partially predicted by underlying white matter connectivity. *Neuroimage*. 2015;108:23-33. doi:10.1016/j.neuroimage.2014.12.033
- Honey CJ, Sporns O, Cammoun L, et al. Predicting human resting-state functional connectivity from structural connectivity. *Proc Natl Acad Sci USA*. 2009;106(6):2035-2040. doi:10.1073/pnas.0811168106
- Wirisch J, Perry A, Ridley B, et al. Whole-brain analytic measures of network communication reveal increased structure-function correlation in right temporal lobe epilepsy. *Neuroimage Clin*. 2016;11:707-718. doi:10.1016/j.nicl.2016.05.010
- Ridley B, Wirisch J, Bettus G, et al. Simultaneous intracranial EEG-fMRI shows intermodality correlation in time-resolved connectivity within normal areas but not within epileptic regions. *Brain Topogr*. 2017;30(5):639-655. doi:10.1007/s10548-017-0551-5

30. Wieser HG, Blume WT, Fish D, et al. Proposal for a new classification of outcome with respect to epileptic seizures following epilepsy surgery. *Epilepsia*. 2001;42:282-286. doi:10.1046/j.1528-1157.2001.4220282.x
31. Horsley JJ, Schroeder GM, Thomas RH, et al. Volumetric and structural connectivity abnormalities co-localise in TLE. *Neuroimage Clin*. 2022;35:103105. doi:10.1016/j.nicl.2022.103105
32. Yeh FC, Wedeen VJ, Tseng WYL. Estimation of fiber orientation and spin density distribution by diffusion deconvolution. *Neuroimage*. 2011;55(3):1054-1062. doi:10.1016/j.neuroimage.2010.11.087
33. Morgan VL, Rogers BP, Anderson AW, Landman BA, Englot DJ. Divergent network properties that predict early surgical failure versus late recurrence in temporal lobe epilepsy. *J Neurosurg*. 2019;132(5):1324-1333. doi:10.3171/2019.1.jns182875
34. Goñi J, van den Heuvel MP, Avena-Koenigsberger A, et al. Resting-brain functional connectivity predicted by analytic measures of network communication. *Proc Natl Acad Sci USA*. 2014;111(2):833-838. doi:10.1073/pnas.1315529111
35. Alstott J, Breakspear M, Hagmann P, Cammoun L, Sporns O. Modeling the impact of lesions in the human brain. *PLoS Comput Biol*. 2009;5(6):e1000408. doi:10.1371/journal.pcbi.1000408
36. Sinha N, Dauwels J, Wang Y, Cash SS, Taylor PN. An in silico approach for pre-surgical evaluation of an epileptic cortex. *Annu Int Conf IEEE Eng Med Biol Soc*. 2014;2014:4884-4887. doi:10.1109/EMBC.2014.6944718
37. Bell GS, de Tisi J, Gonzalez-Fraile JC, et al. Factors affecting seizure outcome after epilepsy surgery: an observational series. *J Neurol Neurosurg Psychiatry*. 2017;88(11):933-940. doi:10.1136/jnnp-2017-316211
38. Sarwar T, Tian Y, Yeo BTT, Ramamohanarao K, Zalesky A. Structure-function coupling in the human connectome: a machine learning approach. *Neuroimage*. 2021;226:117609. doi:10.1016/j.neuroimage.2020.117609
39. Suárez LE, Markello RD, Betzel RF, Misisic B. Linking structure and function in macroscale brain networks. *Trends Cogn Sci*. 2020;24(4):302-315. doi:10.1016/j.tics.2020.01.008
40. Zhang Z, Liao W, Chen H, et al. Altered functional-structural coupling of large-scale brain networks in idiopathic generalized epilepsy. *Brain*. 2011;134(10):2912-2928. doi:10.1093/brain/awr223
41. Astner-Rohracher A, Zimmermann G, Avigdor T, et al. Development and validation of the 5-SENSE score to predict focality of the seizure-onset zone as assessed by stereoelectroencephalography. *JAMA Neurol*. 2022;79(1):70-79. doi:10.1001/jamaneuro.2021.4405
42. Li A, Huynh C, Fitzgerald Z, et al. Neural fragility as an EEG marker of the seizure onset zone. *Nat Neurosci*. 2021;24(10):1465-1474. doi:10.1038/s41593-021-00901-w
43. Proix T, Bartolomei F, Guye M, Jirsa VK. Individual brain structure and modelling predict seizure propagation. *Brain*. 2017;140(3):641-654. doi:10.1093/brain/awx004
44. Betzel RF, Medaglia JD, Kahn AE, Soffer J, Schonhaut DR, Bassett DS. Structural, geometric and genetic factors predict interregional brain connectivity patterns probed by electrocorticography. *Nat Biomed Eng*. 2019;3(11):902-916. doi:10.1038/s41551-019-0404-5
45. Chiang S, Stern JM, Engel J, Haneef Z. Structural-functional coupling changes in temporal lobe epilepsy. *Brain Res*. 2015;1616:45-57. doi:10.1016/j.brainres.2015.04.052
46. Jehi L, Yardi R, Chagin K, et al. Development and validation of nomograms to provide individualised predictions of seizure outcomes after epilepsy surgery: a retrospective analysis. *Lancet Neurol*. 2015;14(3):283-290. doi:10.1016/s1474-4422(14)70325-4
47. Taylor PN, Pappasavvas CA, Owen TW, et al. Normative brain mapping of interictal intracranial EEG to localize epileptogenic tissue. *Brain*. 2022;145(3):939-949. doi:10.1093/brain/awab380
48. Bernabei JM, Sinha N, Arnold TC, et al. Normative intracranial EEG maps epileptogenic tissues in focal epilepsy. *Brain*. 2022;145(6):1949-1961. doi:10.1093/brain/awab480
49. Mercier MR, Dubarry A-S, Tadel F, et al. Advances in human intracranial electroencephalography research, guidelines and good practices. *Neuroimage*. 2022;260:119438. doi:10.1016/j.neuroimage.2022.119438
50. Sinha N, Johnson GW, Davis KA, Englot DJ. Integrating network neuroscience into epilepsy care: progress, barriers, and next steps. *Epilepsy Curr*. 2022;22(5):272-278. doi:10.1177/15357597221101271